Evaluation of multi-user multiple-input multiple-output digital beamforming algorithms in B5G/6G low Earth orbit satellite systems

Received: 30 November 2022 | Revised: 12 April 2023 | Accepted: 20 July 2023

DOI: 10.1002/sat.1493

SPECIAL ISSUE PAPER

WILEY

Evaluation of multi-user multiple-input multiple-output digital beamforming algorithms in B5G/6G low Earth orbit satellite systems

M. Rabih Dakkak[1] | Daniel Gaetano Riviello[1] | Alessandro Guidotti[2] | Alessandro Vanelli-Coralli[1]

[1]Department of Electrical, Electronic, and Information Engineering (DEI), University of Bologna, Bologna, Italy

[2]National Inter-University Consortium for Telecommunications (CNIT), Bologna, Italy

Correspondence
Daniel Gaetano Riviello, Department of Electrical, Electronic, and Information Engineering (DEI), University of Bologna, Bologna, Italy.
Email: daniel.riviello@unibo.it

Funding information
Horizon 2020 Framework Programme; European Union Horizon, Grant/Award Number: 101004145

Summary

Satellite communication systems will be a key component of 5G and 6G networks to achieve the goal of providing unlimited and ubiquitous communications and deploying smart and sustainable networks. To meet the ever-increasing demand for higher throughput in 5G and beyond, aggressive frequency reuse schemes (i.e., full frequency reuse), combined with digital beamforming techniques to cope with the massive co-channel interference, are recognized as a key solution. Aimed at (i) eliminating the joint optimization problem among the beamforming vectors of all users, (ii) splitting it into distinct ones, and (iii) finding a closed-form solution, we propose a beamforming algorithm based on maximizing the users' signal-to-leakage-and-noise ratio served by a low Earth orbit satellite. We investigate and assess the performance of several beamforming algorithms, including both those based on channel state information at the transmitter, that is, minimum mean square error and zero forcing, and those only requiring the users' locations, that is, switchable multi-beam. Through a detailed numerical analysis, we provide a thorough comparison of the performance in terms of per-user achievable spectral efficiency of the aforementioned beamforming schemes, and we show that the proposed signal to-leakage-plus-noise ratio beamforming technique is able to outperform both minimum mean square error and multi-beam schemes in the presented satellite communication scenario.

KEYWORDS
beamforming, beyond 5G, MU-MIMO, satellite communications, 6G

1 | INTRODUCTION

Satellite communication (SatCom) systems are expected to play a crucial role in future wireless networks. The integration of the non-terrestrial network (NTN) component in the terrestrial network (TN) 5G ecosystem, envisaged in 3GPP Rel. 17 and up to Rel. 20 for 5G-Advanced,[1] aims at improving the system flexibility, adaptability, and resilience, as well as extending the 5G coverage to rural, under- or un-served areas.[2,3] Furthermore, the unification of TN-NTN in 6G ecosystems (beyond Rel. 20), as highlighted in Guidotti et al,[1] is expected to achieve further enhancement capabilities, and enable a joint optimization of the fully integrated TN-NTN. SatCom is thus becoming an essential component to efficiently

support the concept of wireless connectivity anywhere, anytime, and at any device. To completely enable this new role of SatCom systems, it is necessary to satisfy the user demand, in terms of different services, such as Internet of Things, and enhanced mobile broadband, characterized by different performance requirements concerning rate and latency. In order to meet the demanding B5G/6G requirements, both academia and industry have been focusing on advanced system-level techniques to increase the offered capacity. One approach is to better exploit the available spectrum, by either adding unused or underused spectrum chunks by means of flexible spectrum usage paradigms (e.g., cognitive radio solutions[4–7]) or by fully exploiting the spectrum by decreasing the frequency reuse factor down to full frequency reuse in multi-beam systems. Notably, the latter solution introduces substantial co-channel interference (CCI) from adjacent beams, thus necessitating the use of advanced interference management techniques, either at the transmitter-side, such as precoding and beamforming,[8–14] or at the receiver, such as multi-user detection.[15–17]

During the last years, the implementation of beamforming techniques in SatCom has been widely addressed for Geostationary Earth Orbit systems, but also for low Earth orbit (LEO) constellations, as reported in the literature[8–14] and the references therein. In these works, the main objective was to increase the overall throughput in unicast and/or multicast systems, also addressing well-known challenges for SatCom-based beamforming as scheduling[18–23] and channel state information (CSI) retrieval.[24] One of the most used techniques to increase the high demand of capacity is Multi-user multiple-input multiple-output (MU-MIMO). The design of hybrid beamforming algorithms for MU-MIMO communications in LEO systems has been recently addressed in Palacios et al.[13]; here, the authors focused on a specific implementation of an on-board beamforming codebook compatible with 3GPP new radio. A thorough survey on MIMO techniques applied to SatCom is provided in Arapoglou et al,[8] where both fixed and mobile satellite systems are examined and the major impairments related to the channel are identified. In the framework of MU-MIMO in SatCom, a critical challenge is the availability of CSI at the transmitter, especially in systems involving non geostationary satellites, as the one considered in this work. Such problem is also further compounded by the mobility of both the user equipments (UEs) and the satellites, which can make the coherence time of the channel shorter than the transmission delay. The effect of non-ideal CSI at the transmitter, when applying beamforming in SatCom, is discussed in Zorba et al,[25] where the authors proposed a novel MIMO scheme aimed at increasing the system sum-rate, availability, and variance performance.

The design of an optimal MU-MIMO beamforming scheme usually pursues the maximization of the output signal-to-interference-plus-noise ratio (SINR) for each user. However, this optimization problem is very well known to be challenging due to its coupled nature and no closed-form solution yet exists. Alternative beamforming schemes, such as the signal to-leakage-plus-noise ratio (SLNR), which are able to transform the coupled optimization problem into a completely decoupled one, have been widely proposed in TNs,[26–29] and recently in NTNs too.[30–33] Lin et al[30] utilized the SLNR metric to address the secure and energy efficient beamforming in multi-beam satellite systems, whereas An et al[31] investigated the secrecy performance of a cognitive satellite-terrestrial network and they introduced hybrid zero forcing (ZF) and partial ZF to solve the optimization problem and obtain the beamforming (BF) weight vectors in a closed form; finally, Lin et al[32] utilized singular value decomposition and uplink-downlink duality to optimize BF vectors for hybrid satellite-terrestrial networks. Vázouez et al[33] investigated the design of a generalized SLNR (G-SLNR) beamformer for multigroup-multicast transmission, that is, they focused on the design of a single SLNR beamformer for a group of users with similar channel coefficients. They target a medium Earth orbit satellite communication system in clear sky propagation conditions. In our paper, we design the transmit beamforming vectors based on the maximization of the SLNR, and we focus instead on a unicast approach for a LEO satellite communication systems considering both line of sight (LOS) and non-line of sight (NLOS) propagation scenarios. The proposed criterion aims at maximizing the received desired signal power for each user, while minimizing the overall interference power caused by each user to all other co-channel receivers. The resulting solution does not impose a restriction on the number of available transmit antennas and it determines the optimal procedure by solving a generalized eigenvalue problem.[34] Furthermore, this scheme, as it has been presented before, aims at splitting the BF optimization problem into distinct ones in order to obtain a closed-form solution. However, to the best of our knowledge, it is the first time to introduce this scheme in LEO satellite system for B5G/6G as an efficient technique to mitigate more the co-channel interference and as a further novelty, the satellite's movement is considered in this work.

The system-level performance of the proposed algorithm is compared with benchmark beamforming schemes based on (i) the CSI knowledge at the transmitter, that is, minimum mean square error (MMSE) and zero forcing (ZF) and (ii) the users' location knowledge at the transmitter, that is, switchable multi-beam (MB) beamforming. Please note that in this paper, we further extend our analysis carried out in Dakkak et al.[35]

The remainder of the work is as follows: Section 2 outlines the system model description and the assumptions, and Section 3 introduces the proposed beamforming schemes. The numerical results and discussion are presented in Section 4, and finally, Section 5 concludes this work.

1.1 | Notation

Throughout this paper, and if not otherwise specified, the following notation is used: bold face lower case and bold face upper case characters denote vectors and matrices, respectively. $(\cdot)^T$ denotes the matrix transposition operator. $(\cdot)^H$ denotes the matrix conjugate transposition operator. $\mathbf{A}_{i,:}$ and $\mathbf{A}_{:,i}$ denote the ith row and the ith column of matrix $\mathbf{A}$, respectively. $\mathrm{tr}(\mathbf{A})$ denotes the trace of matrix $\mathbf{A}$.

2 | SYSTEM MODEL

We consider a single multi-beam LEO satellite at altitude h_{sat} equipped with an on-board planar antenna array with N radiating elements, providing connectivity to K uniformly distributed on-ground UEs by means of S beams. As previously mentioned, full frequency reuse is assumed and, thus, all beams use the same spectral resources. In the framework of NTN, in order to provide connectivity to the users, the LEO Satellite shall always maintain a logical link with an on-ground gNB; to this aim, the satellite is assumed to be either directly connected to an on-ground gateway (GW) or to be connected to other LEO satellites in the constellation by means of inter-satellite links (ISLs). For the scope of this work, the two options are equivalent and are not further discussed in the following. It is worth mentioning that the adopted system architecture is thoroughly described in Guidotti et al.[36] The LEO satellite is assumed to implement digital beamforming techniques. These techniques, detailed in the next section (Section 3), require the estimation of either the CSI or the users' locations provided by the UEs.

As shown in Figure 1, these estimates are computed at a generic time instant t_0 in which the satellite is in a given orbital position. Then, the estimates are provided to the network entity for computing the beamforming coefficients, which in the following is assumed to be at the GW. The computed beamforming coefficients are sent back to the satellite to be used in the BF scheme. Thus, as represented in the architecture of Figure 1, the actual beamformed transmission is performed at a time instant t_1. The latency $\Delta t = t_1 - t_0$ between the channel/location estimation phase and the transmission phase introduces a misalignment between the channel on which the beamforming matrix is computed and the actual channel through which the transmission occurs, which impacts the system performance. This latency can be computed as

$$\Delta t = t_{ut,max} + 2t_{feeder} + t_p + t_{ad} \tag{1}$$

where (i) $t_{ut,max}$ is the maximum propagation delay for the UEs requesting connectivity in the coverage area; (ii) t_{feeder} is the delay on the feeder link, considered twice because the estimates are to be sent to the GW on the feeder downlink and then the beamformed symbols are sent back on the feeder uplink to the satellite; (iii) t_p is the processing delay needed to compute the beamforming matrix; and (iv) t_{ad} includes any additional delay (e.g., large scale loss and scintillation).

It is worth mentioning that the effect of phase variation due to payload chains or different on-board local oscillators can be controlled by using configuration in which a single stable oscillator provides a common reference to the individual frequency converters; this is a common multi-beam satellite architecture as mentioned in Arapoglou et al.[37]

The antenna array model is based on ITU-R Recommendation M.2101-0.[38] The coordinate system for the uniform planar array (UPA) is shown in Figure 2. The planar array boresight direction is defined by the direction of the subsatellite point.

The center of the reference system is on-board the satellite at the center of the antenna array and P denotes the position of the on-ground User Terminal (UT), identified by the direction $(\tilde{\vartheta},\tilde{\varphi})$. In the following, we refer to the user direction in terms of the (ϑ,φ) angles, in which the boresight direction is $(0,0)$ and that allows to easily derive the direction cosines for the considered user as follows: $u = \frac{P_y}{||P||} = \sin\vartheta\cos\varphi$, $v = \frac{P_z}{||P||} = \sin\vartheta\sin\varphi$. We can express the array response of the UPA for the generic direction (ϑ_i,φ_i) as the Kronecker product of the array responses

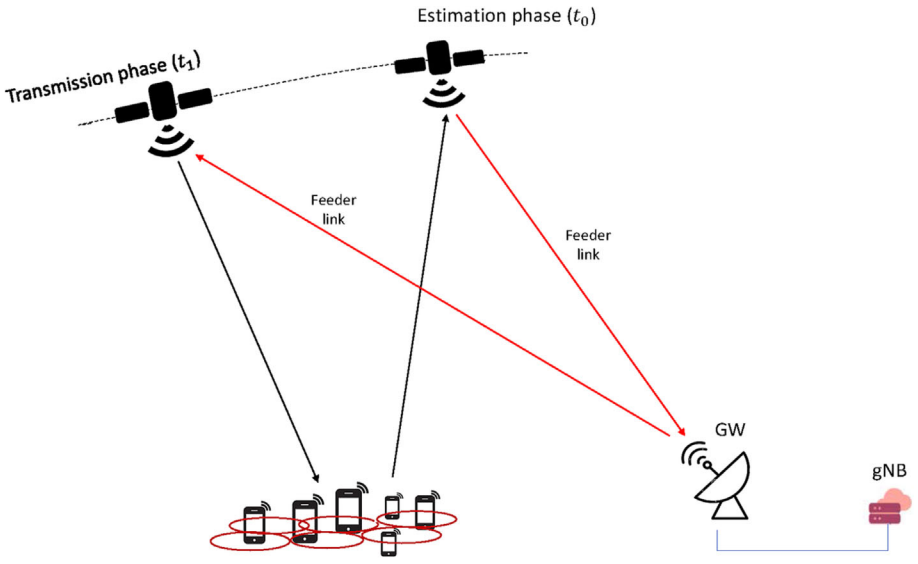

FIGURE 1 System architecture with a single LEO satellite.

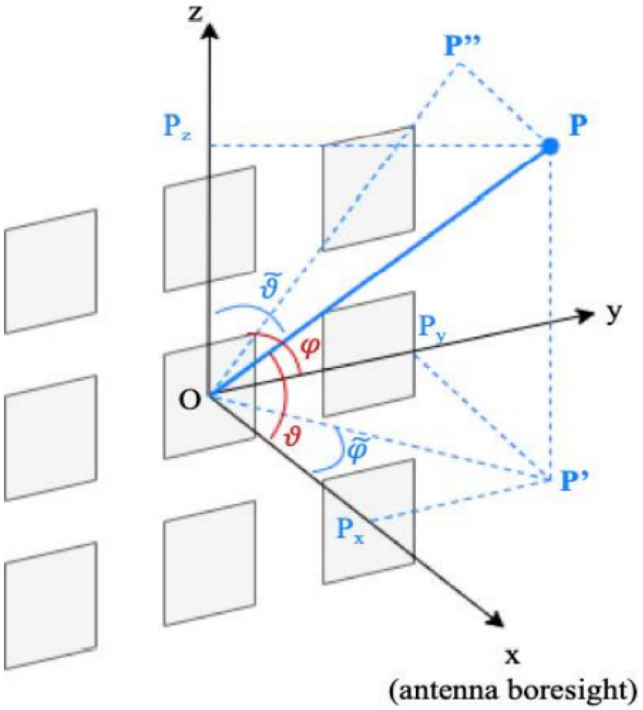

FIGURE 2 Coordinate system for the uniform planar array model.

of the two uniform linear arrays (ULAs) lying on the *y*- and *z*-axis.[22,39,40] Let us first define the $1 \times N_H$ steering vector (SV) of the ULA along the *y*-axis $\mathbf{a}_H(\vartheta_i, \varphi_i)$ and the $1 \times N_V$ SV of the ULA along the *z*-axis $\mathbf{a}_V(\vartheta_i, \varphi_i)$:

$$\mathbf{a}_H(\vartheta_i, \varphi_i) = \left[1, e^{jk_0 d_H \sin\vartheta_i \cos\varphi_i}, \ldots, e^{jk_0 d_H (N_H - 1) \sin\vartheta_i \cos\varphi_i}\right] \tag{2}$$

$$\mathbf{a}_V(\vartheta_i, \varphi_i) = \left[1, e^{jk_0 d_V \sin\vartheta_i \sin\varphi_i}, \ldots, e^{jk_0 d_V (N_V - 1) \sin\vartheta_i \sin\varphi_i}\right]. \tag{3}$$

In the above equations, $k_0 = 2\pi/\lambda$ is the wave number, λ is the wavelength, (N_H, N_V) denote the number of array elements on the horizontal (*y*-axis) and vertical (*z*-axis) directions, respectively, with $N = N_H N_V$ and (d_H, d_V) denote the distance between adjacent array elements on the horizontal and vertical directions, respectively. We assume that the array is equipped with directive antenna elements, whose radiation pattern is denoted by $g_E(\vartheta_i, \varphi_i)$.

Therefore, we can express the total array response, that is, the $(1 \times N)$ SV of the UPA at the satellite targeted for the *i*th user as the Kronecker product of the two SVs along each axis multiplied by the element radiation pattern:

$$\mathbf{a}(\vartheta_i, \varphi_i) = g_E(\vartheta_i, \varphi_i)\, \mathbf{a}_H(\vartheta_i, \varphi_i) \bigotimes \mathbf{a}_V(\vartheta_i, \varphi_i) \tag{4}$$

For the sake of more clarification, it is worth providing the description of the 3-D radiation power pattern $g_{E,\mathrm{dB}}(\vartheta, \varphi)$ of each array antenna element at the satellite,[41,42] which can be expressed in terms of vertical cut $g_{E,\mathrm{dB}}(\vartheta, \varphi = 0^\circ)$ and horizontal cut $g_{E,\mathrm{dB}}(\vartheta = 90^\circ, \varphi)$. The vertical cut is obtained by fixing φ to 0°:

$$g_{E,\mathrm{dB}}(\vartheta, \varphi = 0^\circ) = -\min\left\{12\left(\frac{\vartheta - 90^\circ}{\vartheta_{3\mathrm{dB}}}\right)^2, SLA_V\right\}\ [\mathrm{dB}] \tag{5}$$

with $\theta_{3\mathrm{dB}} = 90^\circ$, $\vartheta \in [0^\circ, 180^\circ]$ and $SLA_V = 30$ dB is the side-lobe attenuation in the vertical direction. The horizontal cut is obtained by fixing ϑ to 90°:

$$g_{E,\mathrm{dB}}(\vartheta = 90^\circ, \varphi) = -\min\left\{12\left(\frac{\varphi}{\varphi_{3\mathrm{dB}}}\right)^2, A_{\max}\right\} \ [\mathrm{dB}] \tag{6}$$

with $\varphi_{3\mathrm{dB}} = 90^\circ$, $\vartheta \in [-180^\circ, 180^\circ]$ and $A_{\max} = 30$ dB the maximum attenuation. The total 3-D radiation power pattern can be finally expressed as

$$g_{E,\mathrm{dB}}(\vartheta, \varphi) = G_{E,\max} - \min\{-(g_{E,\mathrm{dB}}(\vartheta, \varphi = 0^\circ) + g_{E,\mathrm{dB}}(\vartheta = 90^\circ, \varphi), A_{\max}\} \tag{7}$$

where $G_{E,\max}$ is the maximum directional gain of an antenna element and lastly, $g_E(\vartheta, \varphi) = 10^{\frac{g_{E,\mathrm{dB}}(\vartheta,\varphi)}{20}}$.

The CSI vector, $\mathbf{h}_i = [h_{i,1}, \ldots, h_{i,n}, \ldots, h_{i,N}]$, represents the channel between the N radiating elements and the generic ith on-ground UE, with $i = 1, \ldots K$ and can be expressed as

$$\mathbf{h}_i = G_i^{(rx)} \frac{\lambda}{4\pi d_i} \sqrt{\frac{L_i}{\kappa B T_i}} e^{-j\frac{2\pi}{\lambda} d_i} \mathbf{a}(\vartheta_i, \varphi_i) \tag{8}$$

where (i) d_i is the slant range between the ith user and the satellite; (ii) $\kappa B T_i$ denotes the equivalent thermal noise power, with κ being the Boltzmann's constant, B the user bandwidth which is assumed to be the same for all users, and T_i the equivalent noise temperature of the ith user receiving equipment; (iii) L_i denotes the additional losses considered between the ith user and the nth antenna feed (e.g., atmospheric and antenna cable losses), and for a single satellite, we can assume $L_{i,n} = L_i$, $\forall n$; and iv) $G_i^{(rx)}$ denotes the receiving antenna gain for the ith UT. The additional losses are computed as

$$L_i = L_{sha,i} + L_{atm,i} + L_{sci,i} + L_{CL,i} \tag{9}$$

where $L_{sha,i}$ represents the log-normal shadow fading term, $L_{atm,i}$ the atmospheric loss, $L_{sci,i}$ the scintillation, and $L_{CL,i}$ the clutter loss, these terms are computed as per 3GPP TR 38.821[43] and TR 38.811.[44] Collecting all of the K CSI vectors, the system-level $K \times N$ complex channel matrix $\mathbf{H}_{Sys}$ can be built, where the generic ith row contains the CSI vector of the ith user and the generic nth column contains the channel coefficients from the nth on-board feed toward the K on-ground users. During each time frame, the radio resource management algorithm identifies a subset of K_{sch} users to be served, leading to a $K_{sch} \times N$ complex scheduled channel matrix, $\mathbf{H} = \mathcal{F}(\mathbf{H}_{Sys})$, where $\mathcal{F}(\cdot)$ denotes the radio resource management scheduling function, which is a sub-matrix of $\mathbf{H}_{Sys}$, that is, $\mathbf{H} \subseteq \mathbf{H}_{Sys}$, where $\mathbf{H}$ contains only the rows of the scheduled users. The selected beamforming algorithm computes $N \times K_{sch}$ complex beamforming matrix $\mathbf{W}$, which projects K_{sch} dimensional column vectors, $\mathbf{s} = [s_1, \ldots, s_{K_{sch}}]^T$, containing the unit variance user symbols onto the N-dimensional space defined by the antenna feeds. The signal received by the kth user can be expressed as follows:

$$y_k = \underbrace{\mathbf{h}_k \mathbf{W}_{:,k} s_k}_{\text{intended}} + \underbrace{\sum_{i=1, i \neq k}^{K_{sch}} \mathbf{h}_k \mathbf{W}_{:,i} s_i}_{\text{interfering}} + z_k \tag{10}$$

where z_k is a circularly symmetric Gaussian random variable (r.v.) with zero mean and unit variance. The unit variance is motivated by observing that the channel coefficients in (8) are normalized to the noise power. The K_{sch}-dimensional vector of received symbols is

$$\mathbf{y} = \mathbf{H}_{t_1} \mathbf{W}_{t_0} \mathbf{s} + \mathbf{z} \tag{11}$$

It shall be noticed that, as previously discussed, the channel matrix $\mathbf{H}_{t_0}$ is used to compute the beamforming matrix in the estimation phase at time instant t_0, while the beamformed symbols are sent to the users at a time instant t_1, in which the channel matrix is different and denoted as $\mathbf{H}_{t_1}$.

Based on the received symbols, the key performance indicators (KPIs) of each scheduled user in each time frame can be obtained starting from the power transfer matrix as follows:

$$\mathbf{A} = |\mathbf{H}\mathbf{W}|^2 \tag{12}$$

This matrix contains the intended users' power on the diagonal elements, while the off-diagonal elements contain the interference received from each of the other users' signals. Based on **A**, it is possible to compute the received signal-to-noise ratio (SNR) and interference-to-noise ratio as follows:

$$\mathrm{SNR}_k = a(k,k)$$

$$\mathrm{INR}_k = \sum_{i=1, i \neq k}^{K_{sch}} a(k,i) \tag{13}$$

From (13) and (10), the SINR can be computed as

$$\mathrm{SINR}_k = \frac{\mathrm{SNR}_k}{1+\mathrm{INR}_k} = \frac{||\mathbf{h}_k \mathbf{W}_{:,k}||^2}{1+\sum_{i=1, i \neq k}^{K_{sch}} ||\mathbf{h}_k \mathbf{W}_{:,i}||^2} \tag{14}$$

From the above SINR, the spectral efficiency with which each user in each time frame is served can be obtained through the Shannon bound formula (unconstrained capacity) or based on the Modulation and Coding (ModCod) scheme for the considered air interface. In the following, we assume the unconstrained capacity approach, that is,

$$\eta_k = \log_2(1+\mathrm{SINR}_k) \tag{15}$$

3 | DIGITAL BEAMFORMING SCHEMES

In this section, we introduce linear beamforming algorithms focusing on those requiring knowledge of the CSI at the transmitter side, that is, ZF and MMSE, and those requiring the UEs' locations, that is, MB. Moreover, we also design the proposed SLNR-based beamforming algorithm.

ZF and MMSE are known as linear beamforming techniques: ZF can be easily implemented by using the pseudo-inverse of the channel matrix and has optimal performance in high SNR regime; on the contrary, when users experience low SNRs, ZF suffers from noise enhancement and high performance degradation. MMSE overcomes the problem of ZF as it accounts for the noise by adding a regularization factor in its expression. MMSE has indeed much better performance in low SNR regime.

3.1 | Benchmark beamforming algorithms

The following CSI/location based algorithms provide the performance benchmark for the assessment of the proposed SLNR-based beamforming.

3.1.1 | Zero forcing (ZF)

The baseline implementation of the ZF algorithm is based on the inversion of the channel matrix **H**, also known as matched filter beamforming. Notably, with this approach, the $\mathbf{H}^H\mathbf{H}$ matrix is often ill-conditioned, that is, with a very large condition number, leading to a close-to-singular matrix. In these cases, the computation of the inverse matrix is prone to large numerical errors, resulting in a significant performance loss due to the inaccuracy of the matrix inversion; hence, to circumvent this issue, we focus on the following implementation of ZF[45]:

$$\mathbf{W}_{ZF} = (\mathbf{H}^H\mathbf{H})^{\dagger}\mathbf{H}^H \tag{16}$$

where $\dagger$ denotes the Moore–Penrose pseudo-inverse matrix.

It is worth mentioning that ZF scheme suffers from noise enhancement, therefore it may have poor performance in low SNR regime, because it does not take into account the noise power when implementing beamforming vectors. This impacts its performance as reported in the next section of numerical results.

3.1.2 | Minimum mean square error (MMSE)

The MMSE precoder, or regularized zero forcing, is designed to solve the MMSE problem as follows:

$$\mathbf{W}_{MMSE} = \arg\min_{\mathbf{W}} \mathrm{E}||\mathbf{HWs} + \mathbf{z} - \mathbf{s}||^2 \tag{17}$$

$$\mathbf{W}_{MMSE} = \left(\mathbf{H}^H\mathbf{H} + \mathrm{diag}(\boldsymbol{\alpha})\mathbf{I}_N)\right)^{-1}\mathbf{H}^H \tag{18}$$

where $\mathbf{H}$ is the estimated channel matrix. In the above equation, $\boldsymbol{\alpha}$ is a vector of regularization factors, because the channel coefficients are normalized to the noise power, its optimal value[46] is given by $\boldsymbol{\alpha} = \frac{N}{P_t}\mathbf{1}_N$, where P_t is the available transmitted power on the satellite and $\mathbf{1}_N$ is a $N \times 1$ vector of ones. Another aspect worth to be mentioned is that (18) leads to a large dimension of the Gram matrix $\mathbf{H}^H\mathbf{H}$, containing $N \times N$ coefficients. Hence, Icolari et al[4] proposed an alternative formulation that leads to a $K_{sch} \times K_{sch}$ matrix as follows:

$$\mathbf{W}_{MMSE} = \mathbf{H}^H(\mathbf{H}\mathbf{H}^H + \mathrm{diag}(\boldsymbol{\alpha})\mathbf{I}_{K_{sch}})^{-1} \tag{19}$$

The above formulation is computationally efficient because, notably, $K_{sch} < N$.

3.1.3 | Multi-beam (MB)

In this algorithm,[47] the beamforming vectors are computed in an approximated version, that is, a pre-defined codebook of beamforming vectors built by (i) spatially sampling the coverage area, defining a given beam lattice on-ground identified by the beam center locations c_q; $q = 1,\ldots,S$ (as in the example provided in Figure 3) and (ii) computing the beamforming coefficients that are required to form signals with the required spatial signatures, that is, to form beams in these directions. The pre-determined beamforming codebook is to be built as $\mathbf{B} = [\mathbf{b}_1,\ldots,\mathbf{b}_q,\ldots,\mathbf{b}_S]$, where $\mathbf{b}_q$ contains the N-dimensional beamforming vector which is steering the radiation pattern toward the qth beam center. For the generic kth user to be served, its beamforming column vector in the beamforming matrix is identified as the column in the beamforming codebook corresponding to the closest beam center to the kth user's location, that is,

$$\mathbf{W}_{MB} = [\mathbf{W}_{:,1},\ldots,\mathbf{W}_{:,q},\ldots,\mathbf{W}_{:,S}] \tag{20}$$

with

$$\mathbf{W}_{:,k} = \mathbf{B}_{:,j}$$
$$j = \arg\min_{i=1,\ldots,N}||\mathbf{C}_i - \mathbf{P}_k||^2$$

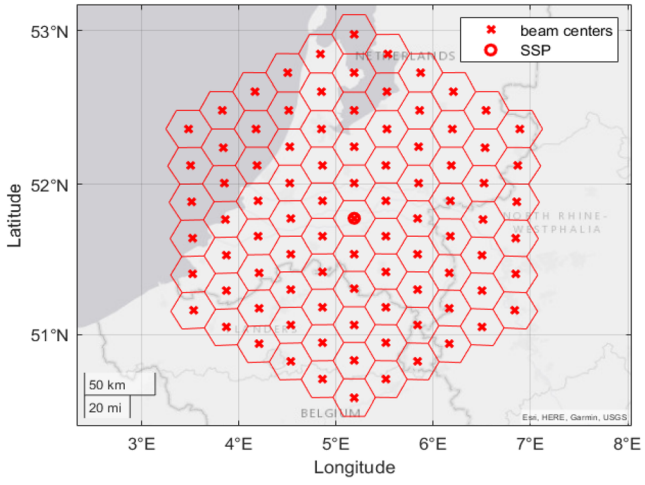

FIGURE 3 Beam lattice in S-band with five tiers.

where $\mathbf{C}_i$ the center of the ith beam and $\mathbf{P}_k$ the position of the kth user. It is worth mentioning that the MB approach is affected by the resolution of spatial sampling: the lower the number of beams, the larger the approximation and, thus, the worse the performance. Finally, it shall be noticed that when one user per beam is selected at each time frame, we obtain $K_{sch} = S$.

3.2 | Proposed SLNR-based beamforming

Given the power transfer matrix in (12), for a given user k, the CCI can be defined as the interference at the user k that is caused by all other users, that is, $\sum_{i,i\neq k} a(k,i)$, while we refer to *leakage* to the interference that user k causes to all other uses, that is, $\sum_{i,i\neq k} a(i,k)$, it can be seen as a measure of how much signal power leaks into the other users. The problem of maximizing the SINR for all users in downlink beamforming has been extensively studied in Schubert and Boche,[48] and no closed-form solutions are available. The specific choice of one user's beamformer may affect the CCI experienced by other users, therefore the SINR values of all users are coupled and the beamformers must be jointly optimized.

In SLNR beamforming, the performance criterion for choosing the beamforming coefficients is based on maximizing the *signal-to-leakage-and-noise ratio* (SLNR) for all users simultaneously. This criterion leads to a decoupled optimization problem and admits an analytical closed-form solution.[34] Unlike ZF scheme, SLNR-based beamforming considers the noise power in implementing beamforming vectors and does not require any dimension condition on the number of transmit/receive antennas. Furthermore, SLNR beamforming can be classified as a regularized channel inversion scheme, with regularization factors customized to each user based on their operating SNR, whereas the MMSE scheme employs the same regularization factor equal to the inverse of average SNR for all users.[49]

In this paper, we consider single stream/layer based-design beamforming, that is, each user terminal is equipped with single receiving antenna. Figure 4 shows the block diagram of the leakage from user 1 on other users, considering a downlink multi-user environment with a single LEO satellite employing N transmit antennas to serve K_{sch} scheduled users.

Considering (14), we note that the power of the desired signal component for user k is given by $||\mathbf{h}_k\mathbf{W}_{:,k}||^2$. At the same time, the interfering power that is caused by the kth user on the signal received by the generic ith user is given by $||\mathbf{h}_i\mathbf{W}_{:,k}||^2$. Thus, we define such quantity, a leakage for user k, as the total power leaked from this user to all other users as follows:

$$\sum_{i=1,i\neq k}^{K_{sch}} ||\mathbf{h}_i\mathbf{W}_{:,k}||^2$$

For each user k, the intended signal power $||\mathbf{h}_k\mathbf{W}_{:,k}||^2$ is aimed to be large compared with the noise power at its receiver, and compared with the power leaked from such user to all other scheduled users, that is, $\sum_{i=1,i\neq k}^{K_{sch}} ||\mathbf{h}_i\mathbf{W}_{:,k}||^2$. These considerations motivate to introduce a figure of merit in terms of SLNR as

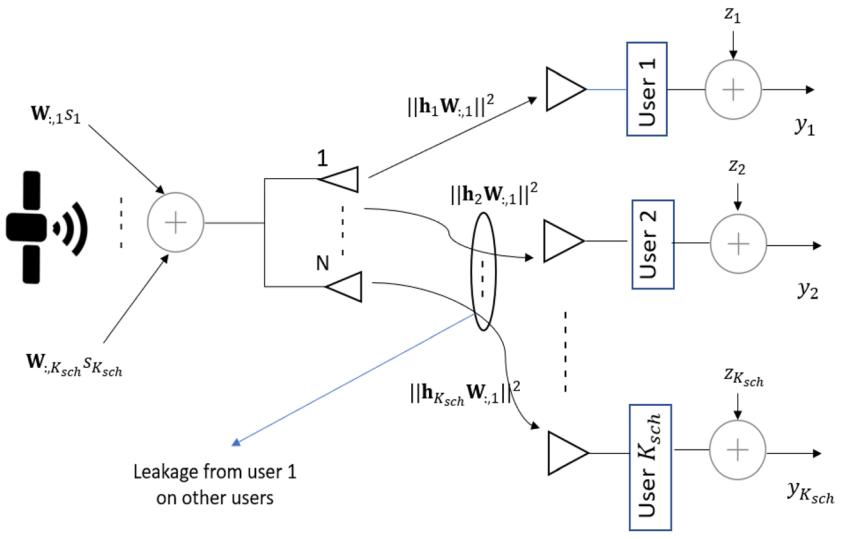

FIGURE 4 Block diagram depicting the leakage from user 1 on other users.

$$\mathrm{SLNR}_k = \frac{||\mathbf{h}_k \mathbf{W}_{:,k}||^2}{\beta + \sum_{i=1, i\neq k}^{K_{sch}} ||\mathbf{h}_i \mathbf{W}_{:,k}||^2} \tag{21}$$

The SLNR expression can be rewritten for the sake of simplicity as

$$\mathrm{SLNR}_k = \frac{||\mathbf{h}_k \mathbf{W}_{:,k}||^2}{\beta + ||\mathbf{Z}_k \mathbf{W}_{:,k}||^2} \tag{22}$$

where

$$\mathbf{Z}_k = [\mathbf{h}_1|...|\mathbf{h}_{k-1}|\mathbf{h}_{k+1}|...|\mathbf{h}_{K_{sch}}]$$

is an extended channel matrix that excludes $\mathbf{h}_k$ only (the vertical bar denotes a vertical concatenation), while $\beta = \frac{K_{sch}}{P_t}$ denotes the SLNR regualarization factor. The beamforming matrix targeted for user k that maximizes its SLNR is given by

$$\hat{\mathbf{W}}_{:,k} = \arg\max_{\mathbf{W}} \mathrm{SLNR}_k = \arg\max_{\mathbf{W}} \frac{||\mathbf{h}_k \mathbf{W}_{:,k}||^2}{\beta + ||\mathbf{Z}_k \mathbf{W}_{:,k}||^2} \tag{23}$$

It is shown in Sadek et al[34] that the optimal beamformer is linked to closed-form solution of the generalized eigenvalue problem:

$$\hat{\mathbf{W}}_{:,k} \propto \max \mathrm{eigenvector}\left\{ (\beta \mathbf{I} + \mathbf{Z}_k^H \mathbf{Z}_k)^{-1} \mathbf{h}_k^H \mathbf{h}_k \right\} \tag{24}$$

In terms of the eigenvector corresponding to the largest eigenvalue of the matrix $(\beta \mathbf{I} + \mathbf{Z}_k^H \mathbf{Z}_k)^{-1} \mathbf{h}_k^H \mathbf{h}_k$, that is, λ_{max}. The column vector $\hat{\mathbf{W}}_{:,k}$ shall be chosen according to (23), which results in the maximum SLNR value, that is,

$$\mathrm{SLNR} = \lambda_{max}$$

In the Table 1, we report the main pros and cons of all benchmark BF schemes as a comparison to the proposed SLNR BF scheme.

Moreover, it is worth providing a comparison regarding the complexity of our proposed scheme with respect to the ideal MMSE BF as follows: the complexity of SLNR BF algorithm could be expressed as $O(K_{sch} N^2 (P + K_{sch} + N + 1))$ where P denotes the number of iterations to find the eigenvector associated with the largest eigenvalue as expressed in (24) by using power iteration algorithm. The complexity of all matrix multiplications and matrix inversion[50] is $O(N^2(K_{sch} + N + 1))$, while the power iteration algorithm has a complexity[51] for each user equals to $O(PN^2)$. Whereas the complexity of MMSE BF can be expressed as $O(K_{sch}^2 N(K_{sch} + 2))$.

Finally, as extensively detailed in Guidotti and Vanelli-Coralli,[11] the power normalization is a fundamental step for beamforming so as to properly take into account the power that can be emitted by both the satellite and per antenna. We consider the following three options for power normalization:

1. The sum power constraint (SPC): an upper bound is imposed on the total on-board power as

TABLE 1 Comparison of BF schemes.

ZF	MMSE	MB	SLNR
✓Good performance in high SNR regime	✓Good performance in both low and high SNR regime	✓Doesn't require CSI knowledge, only users' locations	✓Good performance in both low and high SNR regime ✓Uses a customized regularization factor for each user
× Noise enhancement in low SNR regime	× Requires CSI knowledge	× Approximated scheme	× Requires CSI knowledge
× Requires CSI knowledge		× Poor performance with a small number of beams	× Computationally expensive (requires eigendecomposition for each user)

$$\tilde{\mathbf{W}} = \frac{\sqrt{P_t}\mathbf{W}}{\sqrt{\mathrm{tr}(\mathbf{W}\mathbf{W}^H)}} \tag{25}$$

P_t being the total on-board power, which preserves the orthogonality of the beamformer columns but does not guarantee that the power transmitted from each feed will be upper bounded, that is, it might be working in non-linear regime.

2. Per antenna constraint (PAC): the limitation is imposed per antenna with

$$\tilde{\mathbf{W}} = \sqrt{\frac{P_t}{N}}\mathrm{diag}\left(\frac{1}{||\mathbf{W}_{1,:}||},\ldots,\frac{1}{||\mathbf{W}_{N,:}||}\right)\mathbf{W} \tag{26}$$

However, the orthogonality in the beamformer columns here is disrupted.

3. Maximum power constraint (MPC) solution:

$$\tilde{\mathbf{W}} = \frac{\sqrt{P_t}\mathbf{W}}{\sqrt{N\max_j||\mathbf{W}_{j,:}||^2}} \tag{27}$$

the power per antenna is upper bounded and the orthogonality is preserved, but not the entire available on-board power is exploited. In this framework, it is worth highlighting that with the MB algorithm the three normalization schemes lead to the same beamforming matrix, because the beamforming vectors are normalized by definition.

4 | NUMERICAL RESULTS

In this section, we report the outcomes of the numerical assessment based on the parameters reported in Table 2, considering a single LEO satellite at $h_{sat} = 600$ km. The results are presented in terms of cumulative distribution functions (CDFs) of the users' SINR and achievable spectral efficiency. The UEs are uniformly distributed with a density of 0.5 users/Km^2, which corresponds to an average number of users $K = 28{,}500$ to be

TABLE 2 Simulation parameters.

Parameter	Range
Carrier frequency	2 GHz
System band	S (30 MHz)
Beamforming space	feed
Receiver type	VSAT
Receiver scenario	Fixed, vehicular
Receiver speed, ν_{UE}	(0, 250) km/h
Propagation scenario	LOS, NLOS
System scenario	Urban
User density	0.5 user/km^2
Total on-board power density, $P_{t,dens}$	(1,4,7) dBW/MHz
Number of tiers	5
Number of beams S	91
Number of scheduled users K_{Sch}	91
Number of transmitters N	1024 (32 $\times$32 UPA)
Distance between adjacent array elements $d_H = d_V$	0.55λ
Maximum gain of the antenna element $G_{E,max}$	5.3 dBi
System latency Δt (channel aging)	16.7 ms

Abbreviation: VSAT, Very Small Aperture Terminal.

served for each Monte Carlo iteration. The assessment is performed in full buffer conditions, that is, infinite traffic demand. Based on these assumptions, the users are randomly scheduled. In particular, at each time frame one user for each beam is randomly selected and the total number of time frames is computed so as to guarantee all the users to be served.

The numerical assessment is provided for SLNR-based beamforming and the performance is compared with the benchmark MMSE, ZF, and MB beamforming, assuming ideal CSI/location estimates at the transmitter side. Moreover, by considering Very Small Aperture Terminals (VSATs) as a receiver type, it is worth noticing that it has no advantage related to interference rejection with the directive radiation pattern, because it was supposed that all of the UEs' antennas are pointed toward the single satellite, with the assumption of co-located antenna feeds on the board. We first assume VSATs as fixed terminals and focus on LOS propagation scenario in an urban environment, in which the channel coefficients include free space loss, log-normal shadow fading, atmospheric loss, and scintillation according to 3GPP TR 38.821[43] and TR 38.811.[44]

As mentioned before in the system model description, all the beamforming coefficients are computed through the channel matrix estimated at time instant t_0, while the transmission occurs at time instant t_1, that is, we consider channel aging in our model. Hence, in Table 3, we provide a comparison in the performance of the BF schemes between our case, that is, CSI estimation with channel aging and the case of genie-aided CSI estimation, which means having the ability to estimate the channel coefficients and transmit them at the same time instant. It can be noticed, from the average values of SINR and spectral efficiency in Table 3, a very little degradation in the performance w.r.t. genie-aided CSI case, where for SLNR-SPC the average SINR has been degraded by 1.18 dB and by 1.22 dB for MMSE-SPC.

Figure 5 shows the CDFs of users' SINR and spectral efficiency for all the analyzed beamforming schemes with the SPC and MPC normalization. It is possible to observe that the proposed SLNR-based beamforming provides a better performance than MMSE, followed by ZF and MB, where ZF with SPC shows a better performance with respect to MB. In terms of normalization, SPC is considered the best.

However, SPC does not guarantee that each antenna element or feed does not exceed the power it may emit and, thus, the MPC and PAC solutions could be preferred. However, when comparing them, it can be noticed that the MPC performs significantly better especially when the

TABLE 3 Average performance of BF schemes in case of CSI estimation with channel aging vs. genie-aided CSI estimation.

	BF schemes Genie-aided CSI					
KPIs	**SLNR-SPC**	**SLNR-MPC**	**MMSE-SPC**	**MMSE-MPC**	**ZF-SPC**	**ZF-MPC**
SINR [dB]	22.97	13.80	17.17	11.36	9.92	-1.92
Spectral efficiency [bits/s/Hz]	7.71	4.84	5.80	3.93	3.49	0.84
	CSI with channel aging					
	SLNR-SPC	**SLNR-MPC**	**MMSE-SPC**	**MMSE-MPC**	**ZF-SPC**	**ZF-MPC**
SINR [dB]	21.79	13.48	15.95	10.47	9.56	-1.96
Spectral efficiency [bits/s/Hz]	7.32	4.75	5.41	3.69	3.50	1.1

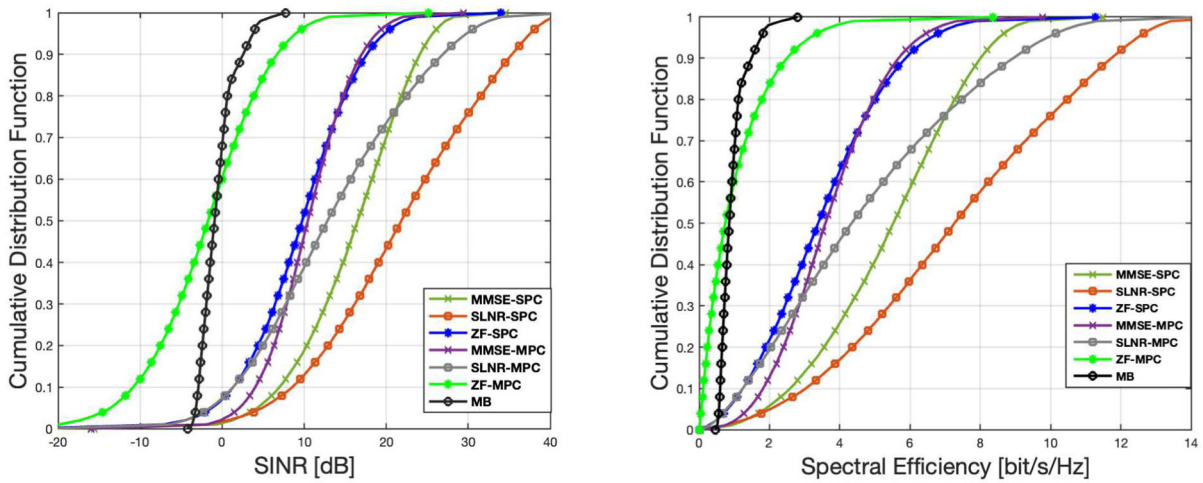

(A) SINR (B) Spectral efficiency

FIGURE 5 CDF of users' SINR and spectral efficiency for fixed VSATs in LOS scenario, at $P_t = 4$ dBW/MHz.

interference in the system is larger, that is, for large values of transmission power and with VSAT terminals that have large antenna gains: in such cases, it is fundamental to maintain the orthogonality in the beamforming matrix columns. Hence, for all beamforming algorithms, PAC provides the worst performance scenario and, thus, we will focus in the analysis only on SPC and MPC normalization.

Figure 6 reports a comparison in the spectral efficiency performance of the SLNR and MMSE beamforming when considering different values of the transmitted power density $P_t = \{1,4,7\}$ dBW/MHz. It can be noted that by doubling the transmitted power for SLNR scheme, we get a gain in the order of 0.7–0.8 bit/s/Hz, and for MMSE in order 0.35–0.45 bit/s/Hz. Such results give additional advantage of superiority of SLNR performance algorithm.

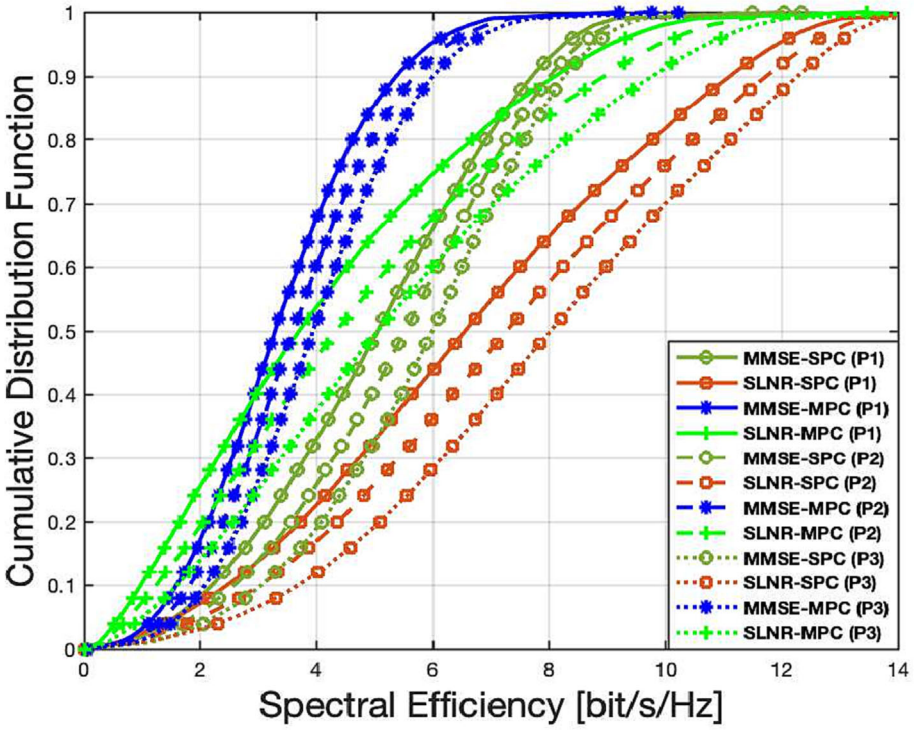

FIGURE 6 CDF of users' spectral efficiency for fixed VSATs in LOS scenario for SLNR and MMSE beamforming with different power density values, $P_1 = 1$ dBW/MHz (solid line), $P_2 = 4$ dBW/MHz (dashed line), and $P_3 = 7$ dBW/MHz (dotted line).

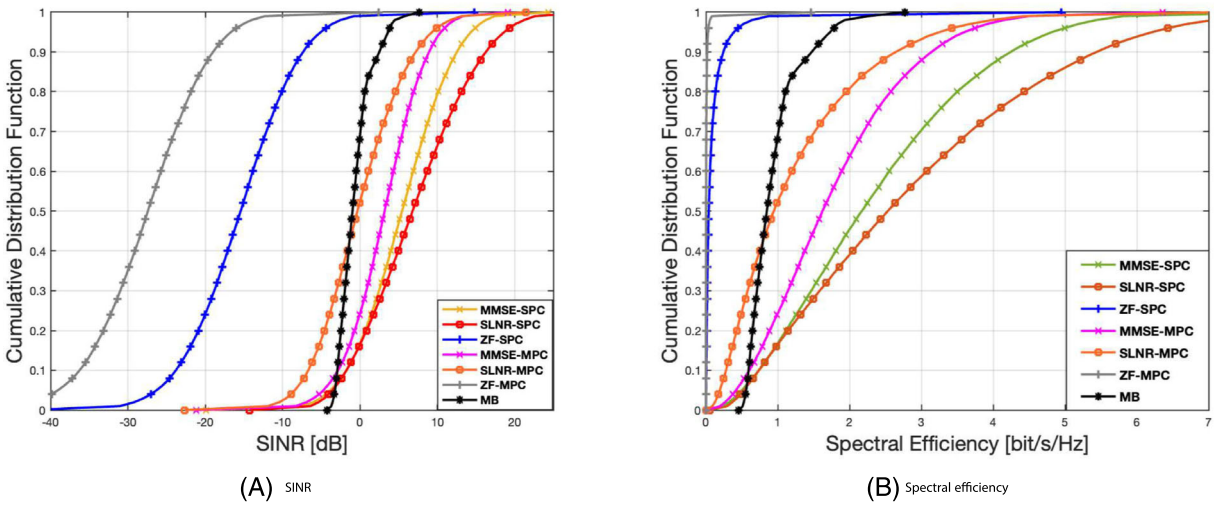

FIGURE 7 CDF of users' SINR and spectral efficiency for fixed VSATs in NLOS scenario with $P_t = 4$ dBW/MHz.

However, the case is different for PAC, a larger transmission power leads to a worse spectral efficiency denoting a significant sensitivity to the loss of orthogonality in the beamforming matrix columns in the increased interference scenario.

We investigate also NLOS propagation conditions in an urban environment. In addition to the channel impairments already present in the LOS scenario, the user experiences clutter loss.[43,44] The distribution of users' SINRs and spectral efficiencies for all the considered beamforming schemes in NLOS scenario for fixed VSATs are reported in Figure 7. It is possible to observe that the proposed SLNR-based beamforming scheme provides again better performance than MMSE, followed by MB. In this case ZF has the worst behavior motivated by its high sensitivity to the shadowing and clutter loss. The superiority of SLNR beamforming over MMSE in both (LOS and NLOS) scenario is motivated by the fact that SLNR uses a customized regularization factor for each user, whereas the MMSE scheme employs the same regularization factor for all of them.[49] This becomes a crucial factor in the presented SatCom scenario, where users experience non-uniform and highly-variable SNRs. Figure 8 shows that the performance significantly gets worse in NLOS conditions compared with the beamforming in LOS scenario, with spectral efficiency degradation in the order of 4–4.5 bit/s/Hz for SLNR-based beamforming and in the order of 3–4 bit/s/Hz for MMSE-SPC and, finally, 1–2 bit/s/Hz for MMSE-MPC. To conclude the assessment of this work, we assess the performance of VSATs when moving at vehicular speed, that is,

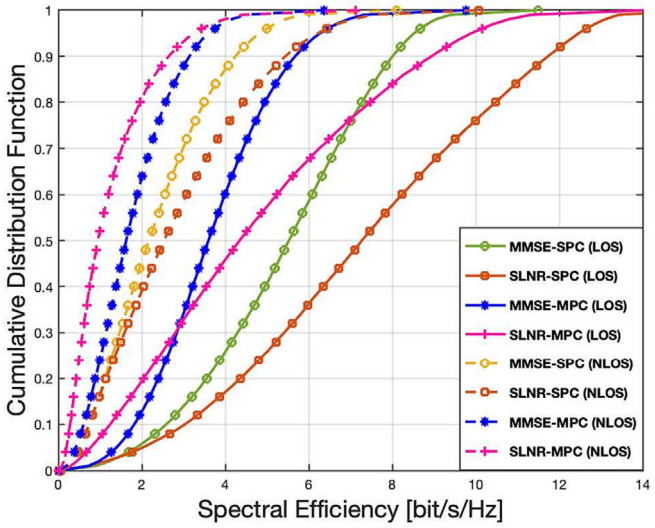

FIGURE 8 CDF of users' spectral efficiency for fixed VSATs and MMSE/SLNR beamforming schemes with $P_t = 4$ dBW/MHz in LOS scenario (solid line) and NLOS scenario (dashed line).

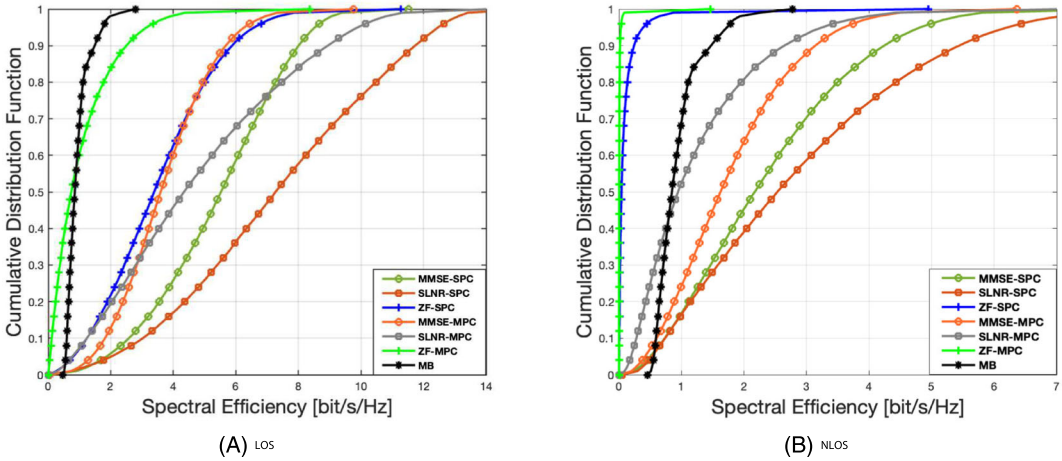

FIGURE 9 CDF of users' spectral efficiency for vehicular VSATs and all considered BF schemes in LOS and NLOS scenarios with $P_t = 4$ dBW/MHz.

at $\nu_{UE} = 250$ km/h as defined in 3GPP TS 22.261.[52] Figure 9 shows the spectral efficiency CDFs for vehicular VSATs considering all the beamforming schemes in LOS and NLOS scenario. It is possible to observe that the proposed SLNR beamforming introduced also higher performance than MMSE followed by MB and ZF.

5 | CONCLUSIONS

In this work, we proposed and assessed a beamforming algorithm in LEO SatCom system based on maximizing the of merit (SLNR) which eliminates the joint coupling between the beamforming vectors into multiple separate optimization problems of the targeting users. We compared its performance to CSI and non-CSI based benchmark algorithms (MMSE and ZF) and MB, respectively. The numerical results provided a significant better performance of SLNR-based beamforming than the optimal MMSE followed by MB and ZF beamforming in terms of spectral efficiency and SINR. The analysis has considered the satellite's movement with both fixed and vehicular VSATs showing a degradation in the performance when moving from LOS to NLOS propagation scenario. As for the normalizations, SPC introduced the best performance for all beamforming algorithms followed by MPC, and PAC was the worst. Finally, the increased transmitted power density introduced slight improvement for SLNR and MMSE beamforming. Future works shall take into account multiple satellites in a mega-constellation scenario targeting global coverage.

ACKNOWLEDGEMENTS

This work has been funded by the European Union Horizon - 2020 Project DYNASAT (Dynamic Spectrum Sharing and Bandwidth-Efficient Techniques for High-Throughput MIMO Satellite Systems) under Grant Agreement 101004145. The views expressed are those of the authors and do not necessarily represent the project. The Commission is not liable for any use that may be made of any of the information contained therein.

ORCID

M. Rabih Dakkak https://orcid.org/0009-0004-2112-3904
Daniel Gaetano Riviello https://orcid.org/0000-0002-7714-9191
Alessandro Guidotti https://orcid.org/0000-0003-4480-0010
Alessandro Vanelli-Coralli https://orcid.org/0000-0002-4475-5718

REFERENCES

1. Guidotti A, Vanelli-Coralli A, Schena V, et al. The path to 5G-advanced and 6G non-terrestrial network systems. In: 2022 11th Advanced Satellite Multimedia Systems Conference and the 17th Signal Processing for Space Communications Workshop (ASMS/SPSC); 2022:1-8. doi:10.1109/ASMS/SPSC55670.2022.9914764
2. Giambene G, Kota S, Pillai P. Satellite-5G integration: a network perspective. *IEEE Netw*. 2018;32(5):25-31.
3. Liu S, Gao Z, Wu Y, et al. LEO satellite constellations for 5G and beyond: how will they reshape vertical domains? *IEEE Commun Mag*. 2021;59(7):30-36.
4. Icolari V, Guidotti A, Tarchi D, Vanelli-Coralli A. An interference estimation technique for satellite cognitive radio systems. In: 2015 IEEE International Conference on Communications (ICC); 2015:892-897.
5. Chatzinotas S, Evans B, Guidotti A, et al. Cognitive approaches to enhance spectrum availability for satellite systems. *Int J Satell Commun Netw*. 2017;35(5):407-442.
6. Liolis K, Schlueter G, Krause J, et al. Cognitive radio scenarios for satellite communications: the CoRaSat approach. In: 2013 Future Network & and Mobile Summit, IEEE; 2013:1-10.
7. Riviello D. Spectrum sensing algorithms for cognitive TV white-spaces systems. *Cognitive communication and cooperative HetNet coexistence*. Springer International Publishing; 2014:71-90. doi:10.1007/978-3-319-01402-9_4
8. Arapoglou P-D, Liolis K, Bertinelli M, Panagopoulos A, Cottis P, De Gaudenzi R. MIMO over satellite: a review. *IEEE Commun Surv Tutorials*. 2010;13(1):27-51.
9. You L, Li K-X, Wang J, Gao X, Xia X-G, Ottersten B. Massive MIMO transmission for LEO satellite communications. *IEEE J Sel Areas Commun*. 2020;38(8):1851-1865.
10. Guidotti A, Vanelli-Coralli A. Clustering strategies for multicast beamforming in multibeam satellite systems. *Int J Satell Commun Netw*. 2020;38(2):85-104.
11. Guidotti A, Vanelli-Coralli A. Design trade-off analysis of beamforming multi-beam satellite communication systems. In: 2021 IEEE Aerospace Conference (50100); 2021:1-12.
12. Guidotti A, Vanelli-Coralli A. Geographical scheduling for multicast precoding in multi-beam satellite systems. In: 2018 9th Advanced Satellite Multimedia Systems Conference and the 15th Signal Processing for Space Communications Workshop (ASMS/SPSC); 2018:1-8.
13. Palacios J, Gonzalez-Prelcic N, Mosquera C, Shimizu T, Wang C-H. A hybrid beamforming design for massive MIMO LEO satellite communications. *Front Space Technol*. 2021;2. [Online]. Available: https://www.frontiersin.org/article/10.3389/frspt.2021.696464
14. Caire G, Debbah M, Cottatellucci L, et al. Perspectives of adopting interference mitigation techniques in the context of broadband multimedia satellite systems. In: ICSSC 2005 23rd AIAA International Communications Satellite Systems Conference; 2005.

15. Colavolpe G, Modenini A, Piemontese A, Ugolini A. Multiuser detection in multibeam satellite systems: theoretical analysis and practical schemes. *IEEE Trans Commun*. 2016;65(2):945-955.
16. Arnau J, Mosquera C. Multiuser detection performance in multi- beam satellite links under imperfect CSI. In: 2012 Conference Record of the Forty Sixth Asilomar Conference on Signals, Systems and Computers (ASILOMAR); 2012:468-472.
17. Christopoulos D, Chatzinotas S, Krause J, Ottersten B. Multi-user detection in multibeam mobile satellite systems: a fair performance evaluation. In: 2013 IEEE 77th Vehicular Technology Conference (VTC Spring); 2013:1-5.
18. Castañeda E, Silva A, Gameiro A, Kountouris M. An overview on resource allocation techniques for multi-user MIMO systems. *IEEE Commun Surv Tutorials*. 2016;20(c):1-1.
19. Chen H, Qi C. User grouping for sum-rate maximization in multiuser multibeam satellite communications. In: ICC 2019 - 2019 IEEE International Conference on Communications (ICC); 2019:1-6. doi:10.1109/ICC.2019.8761875
20. Yi X, Au EK. User scheduling for heterogeneous multiuser MIMO systems: a subspace viewpoint. *IEEE Trans Veh Technol*. 2011;60(8):4004-4013. doi:10.1109/TVT.2011.2165976
21. Storek K, Knopp A. Fair user grouping for multibeam satellites with MU-MIMO precoding. In: GLOBECOM 2017 - 2017 IEEE Global Communications Conference; 2017:1-7. doi:10.1109/GLOCOM.2017.8255098
22. Riviello DG, Ahmad B, Guidotti A, Vanelli-Coralli A. Joint graph-based user scheduling and beamforming in LEO-MIMO satellite communication systems. In: 2022 11th Advanced Satellite Multimedia Systems Conference and the 17th Signal Processing for Space Communications Workshop (ASMS/SPSC); 2022:1-8. doi:10.1109/ASMS/SPSC55670.2022.9914723
23. Ahmad B, Riviello DG, Guidotti A, Vanelli-Coralli A. Graph-based user scheduling algorithms for LEO-MIMO non-terrestrial networks. accepted for publication in 2023 European Conference on Networks and Communications & 6G Summit (EuCNC/6G Summit).
24. Zidane K, Lacan J, Boucheret M-L, Poulliat C. Improved channel estimation for interference cancellation in random access methods for satellite communications. In: 2014 7th Advanced Satellite Multimedia Systems Conference and the 13th Signal Processing for Space Communications Workshop (ASMS/SPSC); 2014:73-77. doi:10.1109/ASMS-SPSC.2014.6934526
25. Zorba N, Realp M, Perez-Neira AI. An improved partial CSIT random beamforming for multibeam satellite systems. In: 2008 10th International Workshop on Signal Processing for Space Communications; 2008:1-8.
26. Sadek M, Aissa S. Leakage based precoding for multi-user MIMO-OFDM systems. *IEEE Trans Wirel Commun*. 2011;10(8):2428-2433. doi:10.1109/TWC.2011.062111.101748
27. Ren B. An improved leakage-based precoding scheme for multi-user MIMO systems. In: 2013 IEEE 77th Vehicular Technology Conference (VTC Spring); Dresden, Germany. 2013;1-4. doi:10.1109/VTCSpring.2013.6691880
28. Riviello DG, Di Stasio F, Tuninato R. Performance analysis of multi-user MIMO schemes under realistic 3GPP 3-D channel model for 5G mmWave cellular networks. *Electronics*. 2022;11(3):330. doi:10.3390/electronics11030330
29. Riviello DG, Tuninato R, Garello R. Assessment of MU-MIMO schemes with cylindrical arrays under 3GPP 3D channel model for B5G networks. In: 2023 IEEE 20th Consumer Communications & Networking Conference (CCNC); Las Vegas, NV, USA. 2023;769-774. doi:10.1109/CCNC51644.2023.10060861
30. Lin Z, An K, Niu H, et al. SLNR-based secure energy efficient beamforming in multibeam satellite systems. In: IEEE Transactions on Aerospace and Electronic Systems; 2022. doi:10.1109/TAES.2022.3190238
31. An K, Lin M, Ouyang J, Zhu W-P. Secure transmission in cognitive satellite terrestrial networks. *IEEE J Sel Areas Commun*. 2016;34(11):3025-3037. doi:10.1109/JSAC.2016.2615261
32. Lin Z, Niu H, An K, Wang Y, Zheng G, Chatzinotas S, Hu Y. Refracting RIS-aided hybrid satellite-terrestrial relay networks: joint beamforming design and optimization. *IEEE Trans Aerosp Electron Syst*. 2022;58(4):3717-3724. doi:10.1109/TAES.2022.3155711
33. Vázouez MA, Artiga X, Pérez-Neira AI. Closed-form multicast precoding for satellite flexible payloads. In: 2021 29th European Signal Processing Conference (EUSIPCO); Dublin, Ireland. 2021:910-914. doi:10.23919/EUSIPCO54536.2021.9616268
34. Sadek M, Tarighat A, Sayed AH. A leakage-based precoding scheme for downlink multi-user MIMO channels. *IEEE Trans Wirel Commun*. 2007;6(5):1711-1721. doi:10.1109/TWC.2007.360373
35. Dakkak MR, Riviello DG, Guidotti A, Vanelli-Coralli A. Evaluation of MU-MIMO digital beamforming algorithms in B5G/6G LEO satellite systems. In: 2022 11th Advanced Satellite Multimedia Systems Conference and the 17th Signal Processing for Space Communications Workshop (ASMS/SPSC); 2022:1-8. doi:10.1109/ASMS/SPSC55670.2022.9914720
36. Guidotti A, Amatetti C, Arnal F, Chamaillard B, Vanelli-Coralli A. Location-assisted precoding in 5G LEO systems: architectures and performances. In: 2022 Joint European Conference on Networks and Communications & 6G Summit (EuCNC/6G Summit); 2022:154-159. doi:10.1109/EuCNC/6GSummit54941.2022.9815611
37. Arapoglou PD, Ginesi A, Cioni S, et al. DVB-S2X-enabled precoding for high throughput satellite systems. *Int J Satell Commun Netw*. 2016;34:439-455.
38. ITU-R Radiocommunication Sector of ITU. Modellingand simulation of IMT networks and systems for use in sharing and compatibility studies. *Recommendation ITU-R M*. 2017:2101.
39. Van Trees HL. *Optimum Array Processing: Part IV of Detection, Estimation and Modulation Theory*. John Wiley & Sons; 2004.
40. Alfano G, Chiasserini C-F, Nordio A, Riviello DG. A random matrix model for mmWave MIMO systems. *Acta Phys Pol B*. 2020;51(7):1627-1640.
41. ITU-R M. Modelling and simulation of IMT networks and systems for use in sharing and compatibility studies; 2101.
42. 3GPP TR 37.840 V12.1.0. Study of radio frequency (RF) and electromagnetic compatibility (EMC) requirements for active antenna array system (AAS) base station (Release 12); 2013.
43. 3GPP. 38.821-solutions for NR to support non-terrestrial networks (NTN); 2021.
44. 3GPP. 38.811 - study on new radio (NR) to support non-terrestrial networks; 2020.
45. Guidotti A, Sacchi C, Vanelli-Coralli A. Feeder link beamforming for future broadcasting services: architecture and performance. In: IEEE Transactions on Aerospace and Electronic Systems. doi:10.1109/TAES.2022.3144243
46. Muharar R, Evans J. Downlink beamforming with transmit-side channel correlation: a large system analysis. In: 2011 IEEE International Conference on Communications (ICC); 2011:1-5. doi:10.1109/icc.2011.5962672
47. Angeletti P, De Gaudenzi R. A pragmatic approach to massive MIMO for broadband communication satellites. *IEEE Access*. 2020;8:132212-132236.

48. Schubert M, Boche H. Solution of the multiuser downlink beamforming problem with individual SINR constraints. *IEEE Trans Veh Technol*. 2004;53(1):18-28.
49. Patcharamaneepakorn P, Armour S, Doufexi A. On the equivalence between SLNR and MMSE precoding schemes with single-antenna receivers. *IEEE Commun Lett*. 2012;16(7):1034-1037. doi:10.1109/LCOMM.2012.050912.120329
50. Li Y, Hu SL, Wang J, et al. An introduction to the computational complexity of matrix multiplication. *J Oper Res Soc China*. 2020;8:29-43. doi:10.1007/s40305-019-00280-x
51. Lin T, Cong J, Zhu Y, Zhang J, Ben Letaief K. Hybrid beamforming for millimeter wave systems using the MMSE criterion. *IEEE Trans Commun*. 2019;67(5):3693-3708. doi:10.1109/TCOMM.2019.2893632
52. 3GPP TS 22.261 V18.2.0. Service requirements for the 5G system; Stage 1 (Release 18); 2021.

AUTHOR BIOGRAPHIES

M.Rabih Dakkak (Graduate Student Member, IEEE) received his BA degree in electronic and telecommunications engineering from University of Aleppo, Syria, in 2014 with academic superiority award. He received his MA degree in telecommunications engineering from the University of Bologna, Italy, in 2020. From 2014 to 2017, he worked as a teaching assistant in RADAR and Microwave Labs at the Faculty of Electronic and Electrical Engineering, University of Aleppo. In 2017, he was awarded the MAECI Scholarship from the Italian government. Currently, he is a PhD candidate at the University of Bologna in the Department of Electrical, Electronic and Information Engineering "Guglielmo Marconi" (DEI). His research focuses on interference management techniques for smart non-terrestrial networks in beyond 5G and 6G systems.

Daniel Gaetano Riviello (Member, IEEE) received his MS in telecommunications engineering (magna cum laude) and his PhD in electronics and communications engineering from Politecnico di Torino, Italy, in 2012 and 2016, respectively. In 2015, he was a visiting researcher at the Centre for Innovation in Telecommunications and Integration of Services (CITI) Laboratory of INSA Lyon, France. He was a postdoctoral research assistant in 2017 with Politecnico di Milano (in collaboration with Huawei Technologies Italia) and from 2018 to 2020 with Politecnico di Torino (in collaboration with TIM). Since 2021, he has been a research fellow with the Department of Electrical, Electronic, and Information Engineering "Guglielmo Marconi," University of Bologna. He has been serving as a TPC member for the EuCNC conference since 2017 and IEEE Globecom since 2022. His research interests focus on wireless communication systems and include massive MIMO and beamforming techniques, array processing and radio resource management for terrestrial and non-terrestrial networks. He is co-recipient of three Best Paper Awards.

Alessandro Guidotti (Member, IEEE) received the master degree (magna cum laude) in telecommunications engineering and the PhD degree in electronics, computer science, and telecommunications from the University of Bologna, Italy, in 2008 and 2012, respectively. From 2009 to 2011, he was a representative for the Italian Administration within CEPT SE43. In 2011 and 2012, he was a visiting researcher at SUPELEC, Paris, France. From 2014 to 2021, he was a research associate with the Department of Electrical, Electronic, and Information Engineering "Guglielmo Marconi," University of Bologna. From 2021, he is a researcher with the Consorzio Interuniversitario delle Telecomunicazioni (CNIT), located at the Research Unit of the University of Bologna. He is active in national and international research projects on wireless and satellite communication systems in several European Space Agency and European Commission funded projects. He is a member of the Editorial Board as Review Editor of the Aerial and Space Networks journal for Frontiers in Space Technologies. He has been serving as TPC and Publication Co-Chair at the ASMS/SPSC Conference since 2018. He is the workshop co-chair of the 2023 IEEE WiSEE Conference and a member of IEEE AESS "Glue Technologies for Space Systems" Technical Panel. His research interests include wireless communication systems, spectrum management, cognitive radios, interference management, 5G, and machine learning.

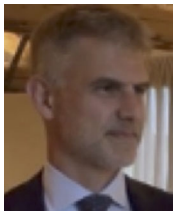

Alessandro Vanelli-Coralli (Senior Member, IEEE) received the Dr. Ing. degree in electronics engineering and the PhD degree in electronics and computer science from the University of Bologna, Italy, in 1991 and 1996, respectively. In 1996, he joined the University of Bologna, where he is currently a full professor. He chaired the PhD board, electronics, telecommunications and information technologies from 2013 to 2018. From 2003 to 2005, he was a visiting scientist with Qualcomm Inc., San Diego, CA, USA. He participates in national and international research projects on wireless and satellite communication systems, and he has been a project coordinator and scientific responsible for several European Space Agency and European Commission funded projects. He is currently the Responsible for the Vision and Research Strategy task force of the Networld2020 SatCom Working Group. He is a member of the editorial board of the Wiley InterScience Journal on Satellite Communications and Networks and associate editor of the editorial board of Aerial and Space Networks Frontiers in Space Technologies. Dr. Vanelli-Coralli has served in the organisation committees of scientific conferences, and since 2010, he is the general CoChairman of the IEEE ASMS Conference. He is a co-recipient of several the Best Paper Awards, and he is the recipient of the 2019 IEEE Satellite Communications Technical Recognition Award.

How to cite this article: Dakkak MR, Riviello DG, Guidotti A, Vanelli-Coralli A. Evaluation of multi-user multiple-input multiple-output digital beamforming algorithms in B5G/6G low Earth orbit satellite systems. *Int J Satell Commun Network*. 2023;1-17. doi:10.1002/sat.1493